Impact of Inverter-based Resources on Impedance-based Protection Functions

Mohammad Zadeh, Prashanth Kumar Mansani
ETAP
Irvine, CA, USA

Ilia Voloh
GE Renewable Energy
Markham, Canada

***Abstract*— Inverter-based resources (IBRs) may inject non-conventional or no negative-sequence current during unbalanced faults. The adverse impact of such fault current characteristic has been reported on fault type identification and directional functions that are essential to impedance-based protection. However, the impact of IBR negative current injection on the core part of different implementations of impedance-based protection function has not been thoroughly investigated. Latest German Gird Code introduces a new requirement for IBRs to inject negative sequence current proportional to its measured negative sequence voltage. In this paper, we will investigate if this requirement can address challenges and issues raised by IBRs for protection relays. This paper investigates and compares the impact of IBRs with two options 1- no negative sequence current injection and 2- negative sequence current injection based on latest German code on phase comparator based methods and impedance-based protection functions. Theoretical analysis, software simulation and commercial relay test have been used for this investigation.**

***Keywords*— Inverter; impedance protection, negative-sequence current injection**

I. INTRODUCTION

Fault current characteristic of inverter-based resources (IBRs) heavily depends on its control logic. Most of the modern inverters only inject positive-sequence current while in some inverter technologies, negative-sequence current is injected to reduce the size of capacitor at the DC side of the inverter. This negative-sequence current does not match with the negative-sequence fault current characteristic of a synchronous machine. As a result, it may result in false trip of protective relays that are designed and operate based on fault current characteristics of synchronous machines.

Recently power industry has realized the importance of injecting negative sequence current by IBR during fault with right characteristics. Latest German Gird Code introduces a new requirement for IBRs to inject negative sequence current proportional to its measured negative sequence voltage [1]. Latest draft of IEEE P2800 [2] also enforces IBRs to inject negative sequence similar to latest German Grid Code. More details of the characteristic of negative sequence current injection required by this code is provided in the paper. Even though the magnitude of IBR fault current is considerably limited as compared to a synchronous machine, the phase angle of positive and negative sequence currents with respect to IBR terminal positive and negative sequence voltages will be similar to a synchronous machine as per latest German code.

Typical impedance-based protection functions depend on 1- fault type identification, 2- fault direction and 3- fault-loop impedance comparison with its corresponding characteristic. The adverse impact of lack or improper IBR negative sequence current injection on fault type identification and directional functions have been discussed in other papers as reported in [3]. Authors assume that these issues can be mitigated either by using different techniques or by new Grid codes that mandate negative-sequence current injection similar to synchronous generators.

Relay vendors have utilized different methods to implement impedance-based protection functions. Some vendors use phase comparators while others measure an impedance to compare against characteristics. The combination of both techniques have been employed as well. This paper first presents implementation of different types of impedance-based protection functions. For each type, the seen impedance equation is derived for performance comparison. Phase comparator-based techniques are also covered as part of the discussion for phase-to-ground fault and phase-to-phase faults. Theoretical and simulation analyses are provided to determine how each method is affected by the lack of negative sequence current from IBR. The performance of each calculation method is compared against the case where the IBR injects negative sequence current as per recent German code [1].

II. DISTANCE PROTECTION

Impedance/Distance protection function is widely used in transmission protection applications due to high speed and reliable operation. In this protection function, positive sequence impedance between relay and fault location is compared directly or indirectly against a characteristic using voltage and current measurements at the relay location. Relay vendors utilize different approaches to implement such protection function. Within microprocessor-based relay technology, from the implementation point of view, it is possible to classify the impedance-based protection function into 1- phase-comparator-based and 2- impedance-measurement-based methods. Each method and its variation are discussed briefly in the following. However, the impact of IBR fault current characteristic particularly lack of negative sequence current is highlighted.

A. Phase-comparator-based Method

In phase-comparator-based method, two signals called polarizing and operating signals are formed out of voltage and current measurements and relay settings. See below.

$$S_{\mathrm{Pol}} = K_1\, V + K_2\, I \tag{1}$$

$$S_{\mathrm{Opr}} = K_3\, V + K_4\, I \tag{2}$$

where, K_1, K_2, K_3 and K_4 are multiplying complex coefficients derived from settings, and V and I are the relay measured voltages and currents.

If the angle of operating signal with respect to polarizing signal falls within a specified range, the comparator output is set to true otherwise false. Different types of characteristics representing the boundary of operation can be created by selecting multiplying coefficients. One or multiple phase comparators can be combined to create impedance-based protection function. Since only the angles of phase comparator signals are used for comparison, the polarizing signal can be selected in such a way to have sufficient magnitude during the fault. In the following, basic implementation of Mho and Quadrilateral ground functions based on the phase comparator technique are presented.

1) Mho characteristic: The basic mho characteristic for phase A is formed by the polarizing and operating signals as shown below.

$$S_{\mathrm{Pol}} = V_{\mathrm{mem1}} \tag{3}$$

$$S_{\mathrm{Opr}} = -V_a + \mathrm{Z}_{\mathrm{Set}}(I_a + \mathrm{K}_0\, I_0) \tag{4}$$

where, V_{mem1} is the positive-sequence memory voltage, $\mathrm{Z}_{\mathrm{Set}}$ is the user reach setting with line angle, K_0 is the zero-sequence compensation factor given by $\mathrm{Z}_0/\mathrm{Z}_1$-1, I_0 is the zero-sequence current and V_a and I_a are the phase A voltage and current [4]. Similar comparators exist for phase B and phase C fault loops.

Phase comparators are widely used for phase-phase fault protection. For BC fault loop, the polarizing and operating signals are given by (5) and (6).

$$S_{\mathrm{Pol}} = V_{\mathrm{mem1\,(bc)}} = -\mathrm{j}\, V_{\mathrm{mem1}} \tag{5}$$

$$S_{\mathrm{Opr}} = -V_{bc} + \mathrm{Z}_{\mathrm{Set}}\, I_{bc} \tag{6}$$

where $V_{\mathrm{mem1\,(bc)}}$ is the line positive-sequence memory voltage for BC loop, and V_{bc} and I_{bc} are line voltage and current for BC loop. The philosophy behind using memory voltage is that the pre-fault and fault voltage angles are very close. This is true for strong sources while for weak sources, there is a considerable phase angle change in relay measured voltage. This angle change results in a well-known dynamic expansion [3] of mho characteristic that increases resistive coverage of the relay in a favorable fashion. This is the case as higher fault resistance is expected for weak sources.

The polarizing and operating signals for the mho relay use phase current and the operation logic is based on Kirchhoff's voltage law. Hence, lack of negative-sequence current from the IBRs do not directly affect the operation of the mho relay. However, as will be shown later through software simulation, the mho characteristic expands less in case of IBR with just positive sequence injection as compared to an IBR with both positive and negative sequence injection based on latest German code.

2) Quadrilateral characteristic: This method is usually employed for detecting ground faults. In a simple form, the quadrilateral ground characteristic can be implemented using four comparators as shown in Table 1. Here, Z_{Rev} is the reverse reach settings, Z_{R} is right blinder characteristic impedance and Z_{L} is the left blinder characteristic impedance. Reverse reactance comparator can be replaced with a phase comparator to create directional quadrilateral ground function. The quadrilateral ground element may use phase current, superimposed phase current, zero-sequence current, or negative sequence current for reactance comparator polarization. Each choice has its pros and cons. Phase current polarization is adversely impacted by the load component. Zero-sequence polarization is adversely impacted by mutual coupling.

Negative sequence is a very common choice in modern protective relaying. IBR non-conventional or no negative sequence current injection results in mal-operation of quadrilateral element based on negative sequence polarization. Further, negative sequence current may be used as a polarizing signal in the directional phase comparator of quadrilateral protection function that in this case is also susceptible to mal-operation.

Table 1 Quadrilateral characteristics comparators

Characteristic	Polarizing signal	Operating signal
Reactance	$\mathrm{j}I_0$ or $\mathrm{j}I_2$	$Z\,(I + \mathrm{K}_0\, I_0) - V$
Reverse reactance	$\mathrm{j}I_0$ or $\mathrm{j}I_2$	$\mathrm{Z}_{\mathrm{Rev}}\,(I + \mathrm{K}_0\, I_0) - V$
Right blinder	$\mathrm{Z}_{\mathrm{R}}\,(I_a + \mathrm{K}_0\, I_0)$	$-V + \mathrm{Z}_{\mathrm{R}}\,(I_a + \mathrm{K}_0\, I_0)$
Left blinder	$\mathrm{Z}_{\mathrm{L}}\,(I_a + \mathrm{K}_0\, I_0)$	$-V + \mathrm{Z}_{\mathrm{L}}\,(I_a + \mathrm{K}_0\, I_0)$

B. Impedance-Measurement (IM)-based Methods

In IM-based approach, first, an impedance or a combination of a reactance and a resistance is estimated. Then, these quantities are compared against a specified characteristic or thresholds defined by user settings. Impedance-measurement-based protection functions are typically used to implement quadrilateral or directional impedance characteristics.

For a fault at distance m from the relay, the voltages seen by the relay for A-to-ground fault and BC fault are given by,

$$V_a = m\mathrm{Z}_1\, I_1 + m\mathrm{Z}_2\, I_2 + m\mathrm{Z}_0\, I_0 + R_{\mathrm{F}}\, I_{\mathrm{F}} \tag{7}$$

$$V_{bc} = mZ_1 I_{bc} + R_F\, I_F \tag{8}$$

where, Z_0, Z_1, and Z_2 are the sequence impedances of the line, I_0, I_1, and I_2 are the sequence currents, I_{F} is the fault current, R_{F} is the fault resistance, and I_{bc} is the phase current. Substituting the zero-sequence compensation factor K_0 (i.e. $\mathrm{Z}_0/\mathrm{Z}_1$-1) in (7) and simplifying yields,

$$V_a = m Z_1\, (I_{\mathrm{a}} + \mathrm{K}_0\, I_0) + R_{\mathrm{F}}\, I_{\mathrm{F}} \tag{9}$$

Apparent impedance estimation methods used by major relay vendors can be broadly classified into four types as outlined below. These four methods are usually employed for phase-to-ground fault, however method III is employed by at least one major relay vendor for phase-phase fault.

1) Method I: In this method, positive-sequence impedance for phase-to-ground fault, mZ_1 is estimated by assuming R_F as zero in (7). Therefore, the estimated impedance mZ_1 is given by:

$$mZ_1 = V_a /(I_a+K_0 I_0) \tag{10}$$

Since this method neglects fault resistance in the calculation, an error is introduced in the estimated impedance given by:

$$\text{Error} = (R_F I_F)/(I_a+K_0 I_0) \tag{11}$$

The error is introduced in both estimated resistance and reactance. Considering typical values for K_0, the estimated fault resistance is considerably less than the actual value. The error is generally approximated as $R_F/(1+K_0/3)$. To compensate for the error, the desired resistive coverage is multiplied with the correction factor when setting the relay to achieve a desired resistive coverage.

2) Method II: Equation (7) can be written as,

$$V_a = mR_1I_R + jmX_1I_X + R_F I_F \tag{12}$$

where $I_R = I_a+ (R_0/R_1\text{-}1)I_0$ and $I_X = I_a + (X_0/X_1\text{-}1)I_0$ in the above equation,

Equating real and imaginary parts of (12),

$$\text{Im}\{V_a\} = mR_1 \text{Im}\{I_R\}+mX_1 \text{Re}\{I_X\}+R_F \text{Im}\{I_F\} \tag{13}$$

$$\text{Re}\{V_a\} = mR_1 \text{Re}\{I_R\}-mX_1 \text{Im}\{I_X\}+ R_F \text{Re}\{I_F\} \tag{14}$$

Solving (13) and (14) for mR1, mX1 yields,

$$mX_1 = \frac{Im\,\{V_a\}\,Re\{I_R\} - Re\,\{V_a\}\,Im\{I_R\}}{Re\{I_X\}\,Re\{I_R\} + Im\{I_X\}\,Im\{I_R\}} - \frac{R_F\,Im\,\{I_F I_R^*\}}{Re\{I_X\}\,Re\{I_R\} + Im\{I_X\}\,Im\{I_R\}} \tag{15}$$

$$mR_1 = \frac{Im\,\{V_a\}\,Im\{I_X\} + Re\,\{V_a\}\,Re\{I_X\}}{Re\{I_X\}\,Re\{I_R\} + Im\{I_X\}\,Im\{I_R\}} + \frac{R_F\,Re\,\{I_F I_R^*\}}{Re\{I_X\}\,Re\{I_R\} + Im\{I_X\}\,Im\{I_R\}} \tag{16}$$

Assuming $\angle I_F \approx \angle I_R$ in (15) and (16) results in,

$$mX_1 = \frac{Im\,\{V_a\}\,Re\{I_R\} - Re\,\{V_a\}\,Im\{I_R\}}{Re\{I_X\}\,Re\{I_R\} + Im\{I_X\}\,Im\{I_R\}} \tag{17}$$

$$mR_1 = \frac{Im\,\{V_a\}\,Im\{I_X\} + Re\,\{V_a\}\,Re\{I_X\}}{Re\{I_X\}\,Re\{I_R\} + Im\{I_X\}\,Im\{I_R\}} + \frac{R_F\,|I_R||I_F|}{Re\{I_X\}\,Re\{I_R\} + Im\{I_X\}\,Im\{I_R\}} \tag{18}$$

The first term of the mR1 given by (19) is used as seen resistance (R_{Seen}) that is impacted by presence of fault resistance.

$$R_{Seen} = \frac{Im\,\{V_a\}\,Im\{I_X\} + Re\,\{V_a\}\,Re\{I_X\}}{Re\{I_X\}\,Re\{I_R\} + Im\{I_X\}\,Im\{I_R\}} \tag{19}$$

Assuming $I_F = I_a$ i.e. there is no feed from the remote end, the approximate error in the estimated resistance can be calculated by

$$R_{SeenError} = R_F/(1+K_r) \tag{20}$$

where, K_r is $(R_0/R_1\text{-}1)/3$. Using the same assumption for resistance estimation, the approximate error in the estimated reactance becomes zero that is advantageous as compared to Method I [5]. Similar to Method I, the fault resistance estimated by this method is smaller as compared to the actual value and the desired resistive coverage is achieved by setting right blinder compensating the expected error defined in (20). Also, phase current is used for impedance estimation so this method is affected by the infeed.

3) Method III: This method is based on a conventional single-ended fault location algorithm for transmission line application [6]. Here the effect of fault resistance R_F is eliminated from the fault loop equation by multiplying it with I_F^*. This method can be employed for phase-to-ground fault and phase-phase fault.

Phase-to-ground loop:

Fault loop equation (7) is multiplie with I_F^* to eliminate the effect of fault resistance R_F as shown below.

$$V_a I_F^*=mZ_1 (I_a +K_0 I_0) I_F^*+R_F I_F I_F^* \tag{21}$$

Equating the imaginary parts on both sides to estimate the fault location,

$$\text{Im}\{V_a\times I_F^*\}=\text{Im}\{(R_1+jX_1)(I_a +K_0 I_0) I_F^*+ R_F |I_F|^2\} \tag{22}$$

Simplifying yields,

$$m=\text{Im}\{V_a\times I_F^*\}/\text{Im}\{(R_1+jX_1)(I_a +K_0 I_0) I_F^*\} \tag{23}$$

From (23), the seen reactance of the relay is given by,

$$mX_1=\text{Im}\{V_a\times I_F^*\}/\text{Im}\{(R_1/X_1 +j)(I_a +K_0 I_0) I_F^*\} \tag{24}$$

Some relays use the following approach to calculate the fault resistance, separately. Equation (7) is multiplied with

$Z_1^*(I_a+K_0I_0)^*$ to eliminate the effect of fault location in the fault resistance as shown below:

$$V_a(Z_1^*(I_a+K_0 I_0))^* = mZ_1(I_a+K_0 I_0)(Z_1^*(I_a+K_0 I_0))^*+R_F I_F (Z_1^*(I_a+K_0 I_0))^* \tag{25}$$

Taking the imaginary parts of (25),

$$\mathrm{Im}\{V_a(Z_1^*(I_a+K_0 I_0))^*\}=R_F\,\mathrm{Im}\{I_F(Z_1^*(I_a+K_0 I_0))^*\} \tag{26}$$

Simplifying yields,

$$R_F = \mathrm{Im}\{V_a(Z_1^*(I+K_0 I_0))^*\}/\mathrm{Im}\{I_F(Z_1^*(I+K_0 I_0))^*\} \tag{27}$$

where, R_F is the estimated fault resistance. The total seen resistance by relay including the faulted section of line and fault resistance is given by,

$$R_{seen} = mR_1+R_F = (mX_1)\times(R_1/X_1) + R_F \tag{28}$$

Several options have been adopted by relay vendors [7][8] to estimate I_F in (24) and (27) such as 1) $3I_0$, 2) $1.5\times I_0 + 1.5\times I_2$, and 3) $3I_2$. For an IBR with non-conventional or no negative sequence current injection, the choice of $I_F = 3\times I_2$ will not be acceptable. As can be seen from (24), the estimated reactance is independent from estimated fault current magnitude. Hence, the choice of $1.5\times I_0 + 1.5\times I_2$ as an estimate of I_F has no considerable impact on the estimated reactance as far as I_2 injected by IBR is zero or small. However, there will be an error on the estimated resistance as the term I_F is only in the denominator.

Phase-to-phase loop:

Equating real and imaginary parts of (8) and solving yields the following equations [9]

$$mX_1=\mathrm{Im}\{V_{bc}\times I_{comp}^*\}\sin\varphi/\mathrm{Im}\{(R_1/X_1+j)I_{bc}I_{comp}^*\} \tag{29}$$

$$0.5R_F = \mathrm{Im}\{V_{bc}(Z_1 I_{bc})^*\}/\mathrm{Im}\{2\,I_{comp}(Z_1 I_{bc})^*\} \tag{30}$$

where, R_F is the estimated fault resistance, I_{comp} is the compensating current and φ is the angle of line impedance. The total seen resistance by the relay is calculated by using (28) and it is used to detect LL as well as LLG faults. Since zero-sequence current is only available for LLG fault, negative sequence current is used to calculate the compensating current, where $I_{comp} = j\sqrt{3}\,I_2$ [9]. Obviously for an IBR with only positive sequence current injection, this method gives an inaccurate result.

4) Method IV: This method is a combination of phase comparator and Method III that is used by at least one of the relay vendors [10]. Here, the seen resistance is calculated using Method III as shown in (28) and reactance is implemented through phase comparator. If negative sequence is not used as polarizing signal in phase comparator, no considerable impact is expected on the reactance reach. The impact on the resistive reach can be inferred by observing the results from Method III.

III. FRT Requirements

Bulk Power System experiences frequency and voltage disturbances during faults. Previously, IBRs are disconnected from the system if disturbances are seen in frequency or voltage. However, with the increasing penetration of renewable resources, fault-ride through (FRT) requirements are mandated to support the grid during disturbances [11].

A. Dynamic Positive Sequence Support (DPS)

Current standards mandate IBRs to support positive sequence current injection during system disturbances. The main objective is to increase the positive sequence voltage by increasing the positive sequence current injection during fault. The operation of the inverter depends on the IBR control mode. IBR control could be operated in real power priority, reactive power priority or power factor control [2] depending upon the setting. In reactive power priority, IBR injects reactive power to maintain the system voltage and IBR may actively curtail the real power to prioritize reactive power injection depending on the deviation in the system voltage. In positive sequence dynamic support, IBRs are in reactive power priority mode and inject positive sequence current depending on the deviation in positive sequence voltage as shown below,

$$I_{q1} = jK_1 \times (|V_{1fault}| - |V_{1pre\text{-}fault}|)\ \angle V_1 \tag{31}$$

where I_{q1} is the positive sequence reactive current injection, K_1 is usually chosen between 2 and 7 and $(|V_{1fault}| - |V_{1pre\text{-}fault}|)$ is typically a negative number. This approach makes IBR to behave like a synchronous generator with $1/K_1$ positive-sequence reactance within its current limits. It is important to note here that for close–in faults IBR reaches its maximum current limit representing smaller effective K_1 factor. IBRs are set to reactive power priority in this study to analyze the impact of DPS on protection functions.

B. Dynamic Positive and Negative Sequence Support (DPNS)

During unbalanced faults, the voltage of the system becomes unbalanced and negative and zero sequence components are introduced into the system. Injecting only positive sequence current results into reactive power injection to all phases including healthy phases. This leads to adverse effects on voltage profile and protection functions as discussed in the later section. Therefore, similar to synchronous generators, it is a preferred to inject both positive and negative sequence currents. Recent German code as shown in Fig. 1 mandates dynamic grid support of positive and negative sequence current for IBRs during unbalanced faults. Positive and negative sequence currents to be injected into the system is calculated based on the FRT curve as shown in (31) and (32). As discussed earlier, the operation of the IBR depends on the control settings. In this study, equal reactive priority is given to the positive sequence injection and negative sequence injection for any disturbances in the system. IBR tries to maximize the positive sequence voltage and minimize the negative-sequence voltage adhering to the short circuit capacity of the converter.

$$I_{q2} = jK_2 \times (|V_{2fault}| - |V_{2pre\text{-}fault}|) \angle V_2 \quad (32)$$

where I_{q2} is negative sequence current injection, K_2 is usually chosen between 2 and 7 and ΔV_2 is typically a positive number. This approach makes IBR to behave like a synchronous generator with $1/K_2$ negative-sequence reactance within its current limits.

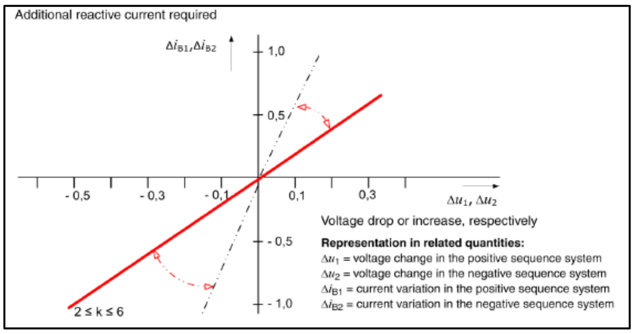

Fig. 1 Germany FRT requirements [1]

IV. Test System Parameters

A test system is created using a 100 MW IBR connected to the grid through a star-delta transformer and 150 KM long transmission line as shown in Fig. 2. As generating stations are connected to the strong point of the grid with low source impedance ratio (SIR), IBR is connected to a grid modeled as voltage source behind a constant impedance with SIR of 0.2. If the current pace in the deployment of renewable energy resources continue, in future most of the generating stations are connected to the grid with high impedances leading to weaker grid. To simulate this scenario, an alternate system is created where the IBR is connected to a weak grid with SIR of 2. The K factor of the IBR is set to 4. As a result, the fault response of the IBR will be similar to a conventional generator with short circuit impedance of 25%. To study the response of DPS and DPNS for an unbalanced fault, a LG, LL and LLG faults are inserted on interconnected transmission line at various fault locations.

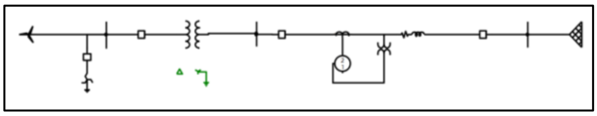

Fig. 2 One-line diagram

V. Power System Impact of DPS Current Injection

The behavior of IBRs with DPS is fundamentally different from a conventional generator. Lack of negative sequence injection from the IBRs affects the system voltage angle, homogeneity etc., principles behind distance protection. Therefore, the impact of DPS on the system voltage and current profile pertain to protection system is studied using the test system in the following section.

A. Voltage profile of unfaulted phases

During line-to-ground fault, IBR with DPS detects the drop in the positive sequence voltage of the system. IBR responds to the disturbance by increasing the positive sequence injection based on FRT requirements to support positive sequence voltage. This supports the faulted phase and increases the voltage as intended. However, since IBR only injects positive sequence voltage, the voltage of the un-faulted phases may increase leading to overvoltage issue. It can be observed in Fig. 3 that during AG fault, the voltage of phase C is raised above 110 % with DPS. On the other hand, IBRs with DPNS inject both positive sequence and negative sequence currents during unbalanced faults. As a result, the behavior of the IBR is similar to conventional generators and un-faulted phases do not experience overvoltage.

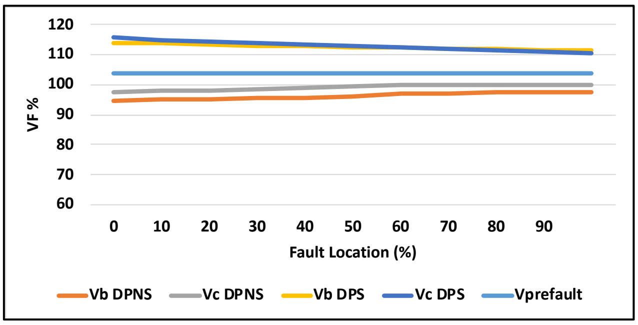

Fig. 3 Voltage of healthy phases during dynamic grid support

B. Change in voltage angle

During close-in faults, voltage drops to about zero leading to mal-operation of self-polarized mho distance function. Therefore, memory polarization is commonly used in microprocessor-based relays to form a polarizing signal. Use of memory voltage polarization results in dynamic expansion of mho characteristic during fault. The degree of dynamic expansion of mho characteristics depends on the system strength. In a strong system, the change in the voltage angle between fault and pre-fault conditions ($\angle V_a - \angle V_{1pre\text{-}fault}$) will be smaller resulting in a smaller expansion. However, in a weak system, the change in voltage angle will be larger leading to a larger expansion of mho characteristic.

IBRs with DPS use full converter capacity to support the positive sequence voltage. Therefore, the change in the voltage angle is small as shown in Fig. 4 resulting in smaller expansion. On the other hand, in IBRs with DPNS, the converter capacity is distributed between maintaining positive sequence voltage and negative sequence voltage by injecting current into the faulted phase(s). Therefore, the angle shift of faulted phase angle is higher as compared to the case of positive sequence support (DPS) as shown in Fig. 5, resulting in larger expansion. This is more prominent in a case where IBR is connected to a weak system.

C. Effect on homogeneity

Impendence-based protection functions need to be properly set to address nonhomogeneous systems. The non-homogeneity creates an angle difference between the current measured by the relay and fault current. The angle difference may adversely impact relay performance if relay is not properly set.

IBRs with DPS do not inject negative sequence current and therefore negative sequence network is open on the IBR side. The negative sequence current at the fault location is supplied by the grid and this creates non-homogeneity in the system as shown in Fig. 6. It can be observed from software simulation that the angle difference of the faulted phase current ($\angle I_{IBR(A)} - \angle I_{Grid(A)}$) is 6° with negative sequence injection while it is 17° without negative sequence injection. Therefore, lack of negative sequence current injection from IBRs with DPS exacerbates the non-homogeneity effect on impedance-based protection function.

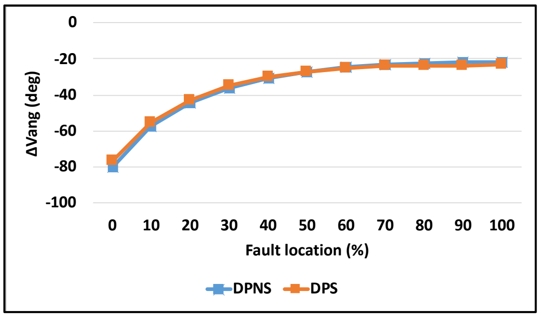

Fig. 4 Voltage angle difference (fault – pre-fault), IBR connected to a strong system

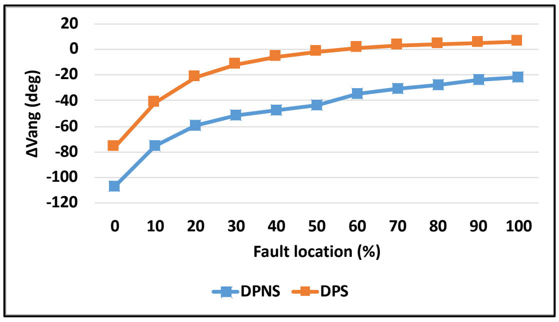

Fig. 5 Voltage angle difference (fault – pre-fault), IBR connected to a weak system

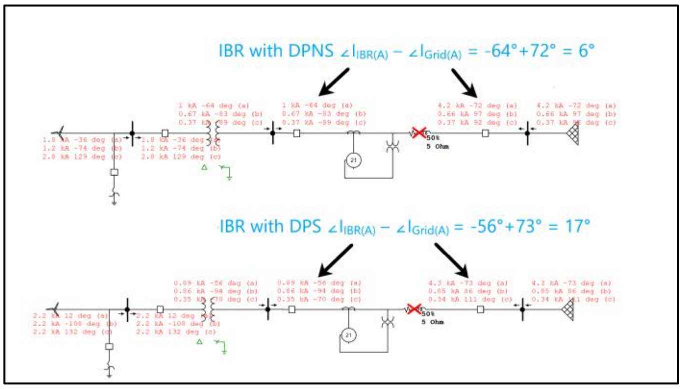

Fig. 6 Effect of DPS and DPNS on the angle difference of the faulted phase

Therefore, it can be concluded that lack of negative-sequence injection results in 1- over-voltage in unfaulted phases, 2- smaller dynamic expansion of memory-polarized Mho characteristic, and greater non-homogeneity seen in currents from both sides feeding a fault.

VI. Simulation and Testing Results

In this section, the impact of DPS and DPNS on different distance protection methods is discussed in detail for both phase-to-ground and phase-to-phase loops.

A. *Phase-to-ground loop*

In this section, the impact of IBRs on phase-comparator based methods and IM-based methods for phase-to-ground fault is discussed.

1) *Phase-comparator-based method*

A phase comparator is modeled with positive sequence memory polarization. As explained in the earlier section, the dynamic expansion of mho characteristics depends on the system strength. IBR with DPS can utilize full converter capacity at disposal to support positive sequence voltage as discussed earlier. Therefore, the dynamic expansion of mho characteristics is expected to be smaller in positive sequence support as compared to the combined positive and negative sequence support. In a strong system, the change in the voltage angle is small. As a result, the resistive coverage of positive sequence support and positive and negative sequence support is almost similar as shown in Fig. 7.

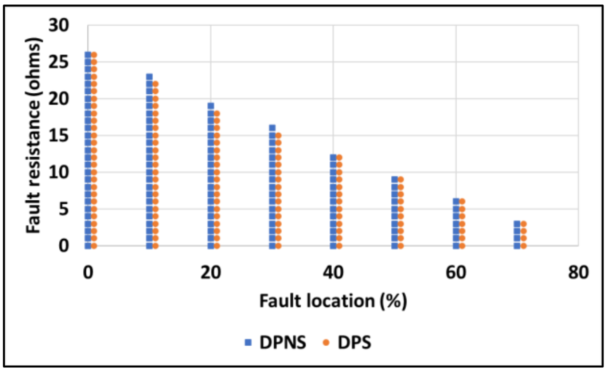

Fig. 7 Expected trip for LG fault in a strong system

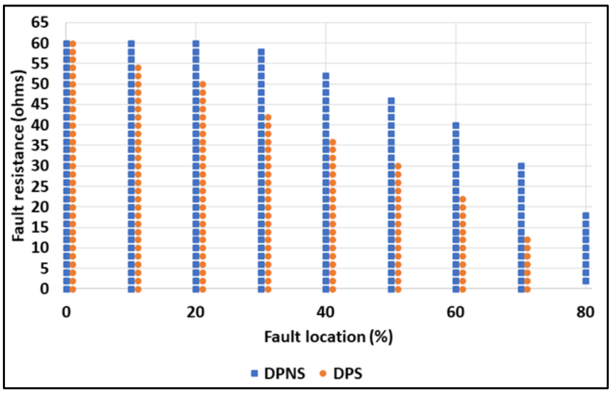

Fig. 8 Expected trip for LG fault in a weak system

For an IBR connected to a weak system, the change in the voltage angle as compared to the memory voltage is considerable as shown in Fig. 5. As predicted in Section V.B and shown in Fig. 8, the resistive coverage in DPS is smaller as compared to the IBR with DPNS. In other words, the Mho characteristic expands less when IBR only injects positive sequence as compared to a case where both positive and negative sequence is injected.

In order to further verify the results of simulation, COMTRADE files were generated for phase-to-ground fault for the case of 60 % fault location and played back as an input to

GE D60 distance relay [12]. The fault resistance is chosen as 15, and 20 ohms for DPS and 35 and 40 ohms for DPNS to generate COMTRADE files. From Table 2, it can be inferred that the resistive reach in DPS is around 15-20 whereas in DPNS it is around 35-40. Therefore, it can be concluded that the resistive reach of the relay in DPS is smaller as compared to the IBR with DPNS. It is important to note that the hardware test results match the simulation results.

Table 2. Actual relay output to play-in COMTRADE cases

IBR injection	Fault location (from IBR)	RF	Expected Trip (ETAP)	Relay output
DPNS	60	35	Yes	Yes
DPNS	60	45	No	No
DPS	60	15	Yes	Yes
DPS	60	25	No	No

2) *Impedance-Measurement-based (IM-based) Methods*

The estimated impedances for Methods I to III are compared with the actual fault impedance to study the impact of IBR as shown below,

$$\Delta R_{\text{seen}} = R_{\text{seen}} - R_{\text{F}} \tag{33}$$

$$\Delta X_{\text{seen}} = X_{\text{seen}} - X_{\text{F}} \tag{34}$$

where, R_{seen} and X_{seen} correspond to the impedance seen by the line relay at the IBR side and R_{F}, X_{F} represent the actual fault impedance. For line-to-ground fault as mentioned in Section II, Method IV is a combination of Method III and phase comparators, thereby the results can be inferred from each one.

Fig. 9 shows the error in seen resistance of all studied methods for a case of IBR connected to a strong system. As it is shown, Method I is not considerably affected. For Method II and Method III where $3\times I_0$ is selected as I_{F}, seen resistances are not affected as expected by the presence or lack of negative sequence current. As predicted in Section II.B.3), the error in the estimated resistance is considerable for Method III with ($1.5\times I_0 + 1.5\times I_2$) as I_{F}. Lack of negative sequence current (DPS) results in higher seen resistance error as compared to the case IBR injects both positive and negative sequence currents (DPNS).

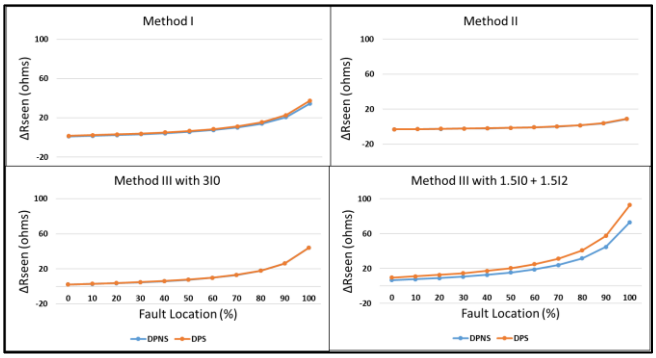

Fig. 9 ΔR_{seen} for LG fault in a strong system at R_f = 5 ohms

Fig. 10 shows the error in seen resistance of all studied methods for a case of IBR connected to a weak system. As expected, due to a smaller feed from the grid side, the overall seen resistance error is considerably smaller as compared to a strong system. In addition, as expected, Method II and Method III with $3I_0$ choice are not impacted by the choice of negative sequence current injection.

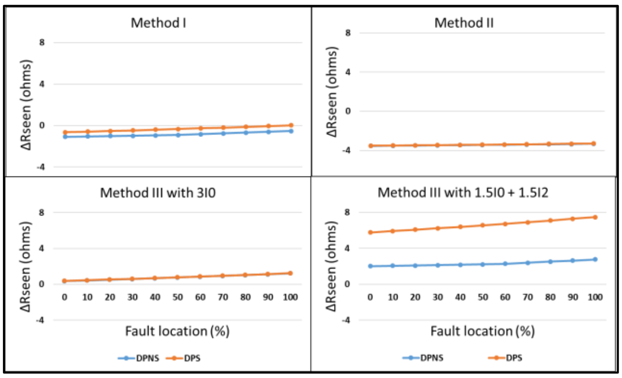

Fig. 10 ΔR_{seen} for LG fault in a weak system at R_f = 5 ohms

The impact of negative sequence current injection on the estimated reactance for strong and weak systems is shown in Fig. 11 and Fig. 12, respectively. As it is shown, the choice of negative sequence current injection does not have any considerable adverse impact on the seen reactance estimation specially for the case where IBR is connected to a strong system.

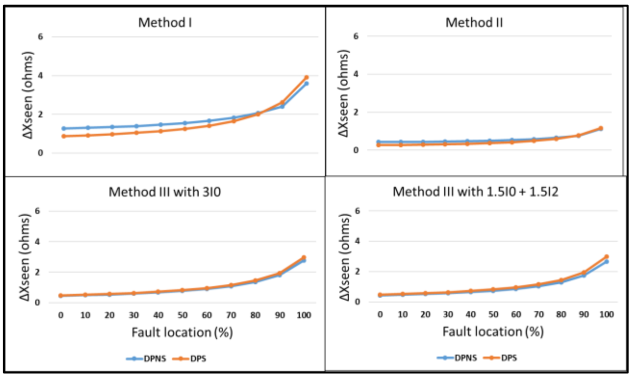

Fig. 11 ΔX_{seen} for LG fault in a strong system at R_f = 5 ohms

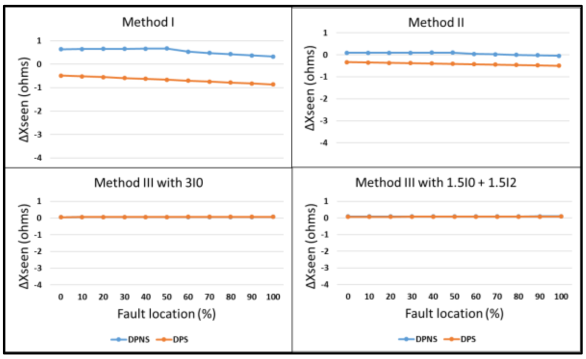

Fig. 12 X_{seen} for LG fault in a weak system at R_f = 5 ohms

B. *Phase-to-phase loop*

The impact of IBRs on phase-to-phase fault loop for phase comparator-based and Method III is discussed in the following section.

1) Phase-comparator-based method

For LL faults, as shown in Fig. 13 and Fig. 14, the dynamic expansion of mho characteristic results in increased resistive coverage similar to LG faults. In weak systems, the change in voltage angle results in increased resistive coverage. However, in strong systems, the change in the voltage angle is small. Therefore, the increase in resistive reach is relatively smaller.

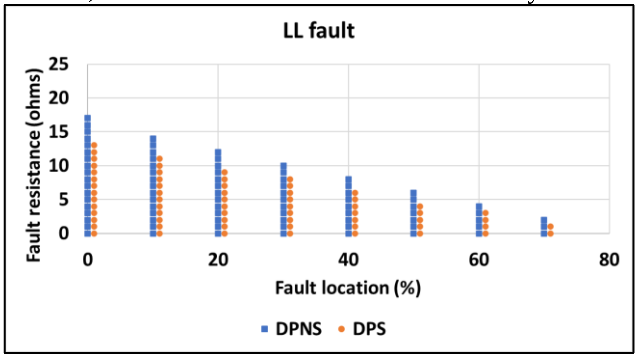

Fig. 13 Expected trip for LL fault in a strong system

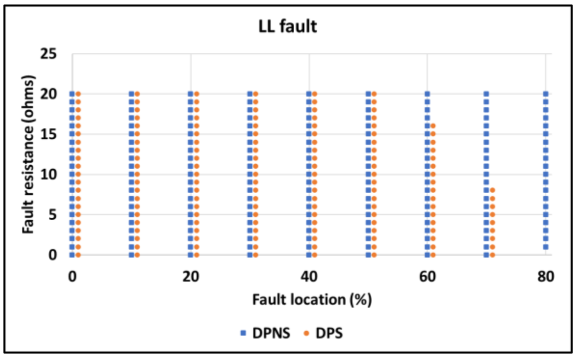

Fig. 14 Expected trip for LL fault in a weak system

For a LLG fault, the fault resistance simulated is between the ground and the joint of faulted phases at the point of fault location. This means that the phase to phase fault loop is not affected by the fault resistance. As a result, large resistive coverage is expected and seen for LLG faults (Fig. 15 and Fig. 16) and the reach of the relay is as set irrespective of the fault resistance.

2) Impedance-Measurement-based (IM-based) Methods

As discussed in Section II, this method directly employs negative sequence current for impedance estimation, as a result gives incorrect results for DPS. Use of this method for the protection of interconnection of IBR to grid should be avoided. Since there is no point of showing these results, there is no comparison can be done as well with the performance of Method III for the case of IBR injecting both positive and negative sequence currents, i.e. DPNS. However, expected trip results for DPNS are provided in Fig. 17 - Fig. 20 with resistive reach setting as 20 ohms. For LL fault, as it is illustrated in Fig. 17 and Fig. 18, the resistive reach is reduced by infeed from the grid end. In strong systems, resistive coverage is adversely impacted by the infeed. However, in weak systems, the relay performance is not affected. For LLG fault, relay trips as set regardless of the fault resistance in both strong and weak systems.

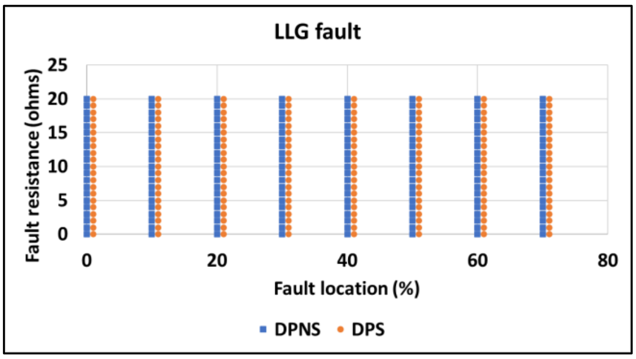

Fig. 15 Expected trip for LLG fault in a strong system

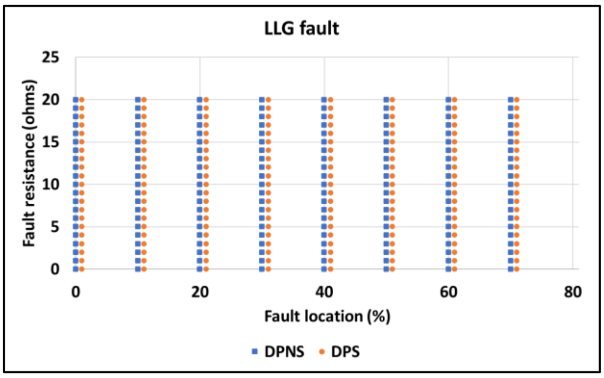

Fig. 16 Expected trip for LLG fault in weak system

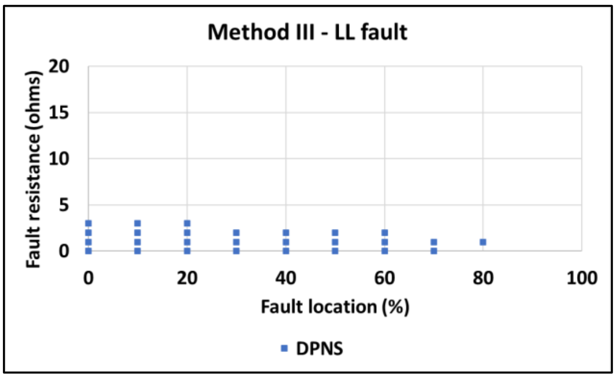

Fig. 17 Expected trip for LL fault in a strong system

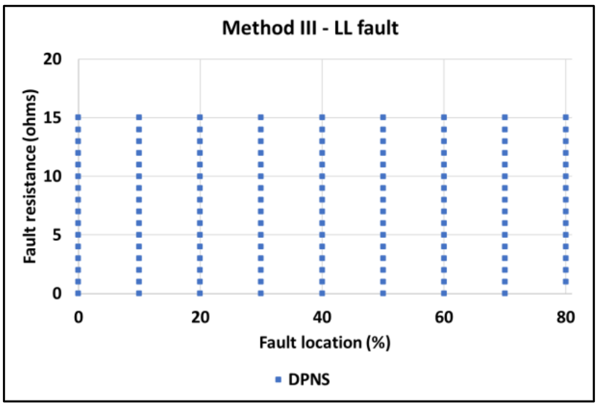

Fig. 18 Expected trip for LL fault in weak system

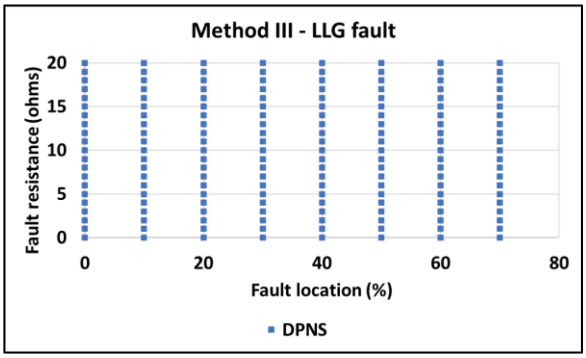

Fig. 19 Expected trip for LLG fault in a strong system

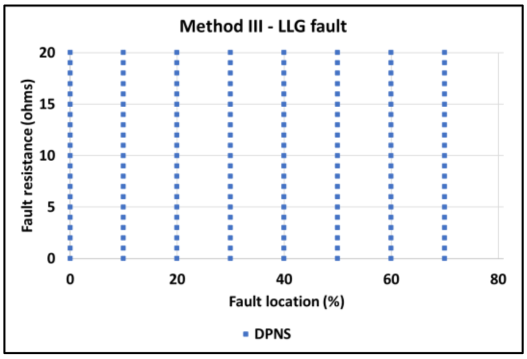

Fig. 20 Expected trip for LLG fault in weak system

VII. Conclusion

Inverter-based resources (IBRs) may inject non-conventional or no negative-sequence current during unbalanced faults. Common commercial techniques used to implement impedance-based protection functions were discussed in this paper. The effect of IBRs with and without negative-sequence injection on impedance-based protection function was investigated. The results for a phase-to-ground faults were validated by testing a commercial relay with software generated COMTRADE files.

Lack of injecting negative sequence current by IBR is found to 1) cause over-voltage in unfaulted phases 2) exacerbate the non-homogeneity effect on impedance-based protection function and 3) result in smaller dynamic expansion of Mho characteristic. Table 3. summarizes the results of simulation and hardware test for the case of no positive sequence current injection (DPS) with respect to the case where both positive and negative sequence current (DPNS) is injected by IBR.

Table 3. Summary of results of DPS vs DPNS

Method	LG	LL	LLG
Phase comparator (Mho)	Smaller resistive coverage	Smaller resistive coverage	Not affected
Method I	Not affected	NA	NA
Method II	Not affected	NA	NA
Method III with $3I_0$	Accurate thought zero-sequence coupling is not studied	NA	NA
Method III with $3I_2$	Shall be avoided	Shall be avoided	Not affected
Method III with $1.5I_0+1.5I_2$	Adversely impacted	NA	NA

References

[1] "Summary of the draft VDE-AR-N 4120," May 2017.

[2] A. Rajapakse, R. Majumder, S. G. R. Energy and R. Nelson, "Modification of commercial fault calculation programs for wind turbine generators," 2020. [Online]. Available: https://www.pes-psrc.org/kb/published/reports/C24_WG_Report_Jun_2020_Final.pdf

[3] "Impact of inverter-based resources on protection schemes based on negative sequence components," EPRI, 2019.

[4] Donald D. Fentie, "Understanding the dynamic mho distance characteristic," Proc. 69th Annual Conf. for Protective Relay Engineers, College Station, Texas, USA, April, 2016, pp. 1-15.

[5] G. Ziegler, "Mode of operation," in *Numerical distance protection: principles and applications*, John Wiley & Sons, 4th edn. 2011, pp. 104-105.

[6] Schweitzer III, O. Edmund, and Jeff Roberts, "Distance relay element design," Proc. 46th Annual Conf. for Protective Relay Engineers, College Station, TX. 1993.

[7] *MiCOM P441/P442 & P444 Numerical Distance Protection*, Schneider Electric, 2011.

[8] *Line distance protection REL650, Version 1.3 IEC, Technical manual*, ABB, 2013.

[9] *SIPROTEC 5, Distance and Line Differ-ential Protection, Breaker Management for 1-Pole and 3-Pole Tripping 7SA87, 7SD87, 7SL87, 7VK87*, Siemens, 2018.

[10] *SEL-421-4, -5, Protection, Automation and Control System, Instruction Manual*, Schweitzer Engineering Laboratories, 2017.

[11] US Federal Energy Regulatory Commission. "Standard interconnection agreement for wind energy," Docket No. RM05-4-000 (2005).

[12] *D60 Line Distance Relay, Instruction Manual*, GE, 2006.